REENTRY PREDICTION OF DEBRIS RISK OBJECTS: LESSONS LEARNT FROM PION

R. Crowther

Space and Communications Department, DRA Farnborough, United Kingdom

ABSTRACT

The trajectories of the PION 5 and 6 satellites released on September 1 and 2 1992 are analysed up to their reentry on 24 September 1992. The orbit data is used for reentry predictions and for the determination of the neutral atmospheric density encountered by the satellites. The influence of short lived geomagnetic storms on the lifetime predictions is discussed and recommendations are made to account for these effects in future reentry prediction campaigns. The neutral density of the atmosphere is seen to vary by almost an order of magnitude during the storms but it is seen to have only a transient effect on the satellite trajectories and a minimal influence on orbital lifetime.

1. INTRODUCTION

The launch on 19 August 1992 of the Resurs-F 16(1992-56A) satellite and the subsequent release of the PION 5(1992-56C) and PION 6(1992-56D) sub-satellites on 1 and 2 September 1992 provided the international tracking community with a rare opportunity to measure its Earth satellite reentry prediction capability against targets of known dimensions, shape and mass. The reentry prediction of debris *risk objects*, artificial satellites such as Skylab(1973-27A) (Ref. 1) and Salyut 7(1982-33A)/Kosmos 1686(1985-86A) (Ref. 2) with in-orbit masses of 75 and 40 tonnes respectively, is normally an imprecise art. In order to accurately predict the rate of orbital decay as the atmosphere exerts an increasing drag force on the satellite, the shape, size, mass and orientation of the relevant satellite must be known in addition to the neutral density of the atmosphere that the satellite encounters along its trajectory.

The term debris implies a redundant, uncontrolled satellite and in practice the configurational characteristics and intrinsic motion of the *risk object* is not well known. Fortunately in the case of the Salyut 7/Kosmos 1686 space station, radar signature analysis by FGAN (Ref. 3) gave a clue to the motion of the complex as it approached it terminal trajectory. Observations suggested a slow transition from a gravity gradient stabilised orientation to a complex tumbling motion as destabilising aerodynamic moments and forces increased. Unfortunately this information is not available in real time and on an operational basis.

The atmosphere of the Earth in the thermospheric region pertinent to satellite reentry prediction is difficult to characterise. The neutral density of the atmospheric species is governed by the thermospheric temperature which shows a marked rise from about 200 K at 100 km to a value between 600 K and 2000 K at 250 km, and then remains constant with altitude. Above 200 km solar-terrestrial interactions influence the atmosphere. First the temperature of the thermosphere varies during the day, mirroring the smaller amplitudes within the troposphere (below 10 km). The second and more dominant influence is due to the extreme ultraviolet radiation produced by the Sun. This varies with the 11 year cycle of sunspot activity with higher temperatures during periods of high activity as the atmosphere absorbs the higher levels of radiation. In addition to varying with this temperature the neutral density is also subject to variation with altitude due to hydrostatic considerations. The behaviour predicted by the CIRA 72 model (Ref. 4) is shown in figure 1. In addition to the long term variations solar activity also produces sharp short-term increases in density. Solar storms which disrupt the Earth's magnetic field can cause transient increases in neutral density by an order of magnitude. Two indices, the solar radiation energy at a wavelength of 10.7 cm, $F_{10.7}$ and the geomagnetic planetary index, a_p show good correlation with the density changes. A semi-annual variation of density is also observed, the amplitude of which is difficult to predict from one year to the next. In addition to these global variations, King-Hele (Ref. 5) reports a general variability in the density of $\approx 10\%$ due to localised and very short term influences.

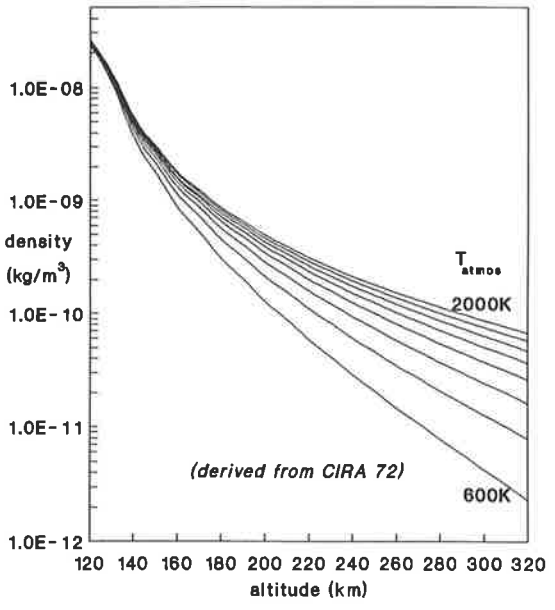

Figure 1. Density variation with temperature and altitude

These uncertainties in *risk object* characteristics and density variations have led to the development of a reentry prediction technique which is independent of these parameters. The *rate of change of mean motion* technique (Ref. 5) pioneered by King-Hele uses direct observations of the past trajectory evolution to imply the values of these parameters and thereby predict the future orbital decay rate and lifetime. An assessment of the performance of this technique for predicting the reentry epoch of the two PION satellites will be presented

in this paper and the lessons that can be learnt in applying the technique to future *risk objects* will be discussed.

2. RATE OF CHANGE OF MEAN MOTION METHOD

This technique has been well documented in a number of papers (Refs. 6 and 7) and the reader is advised to consult these publications for background on the theoretical development. In applying the technique to the PION reentry prediction campaign, we will restrict our attention to the circular orbit case which permits simplification of the orbital theory applied. King-Hele has shown that for a satellite moving in a nominally circular orbit within a static, spherically symmetric atmosphere the remaining orbital lifetime, L (days) is given by:

$$L = \frac{3 H_H n \left(1 - \exp\left(\frac{a_L - a_c}{H}\right)\right)}{2 a \dot{n}} \qquad (1)$$

where n is the mean motion of the orbit (rev/day)
a is the semimajor axis of the orbit (km)
H is the neutral density scale height (km)
H_H is the scale height H km below the minimum altitude of the trajectory (km)

and the subscripts c and L refer to the current semimajor axis value and that at which the satellite reenters ($\approx$120 km) respectively.

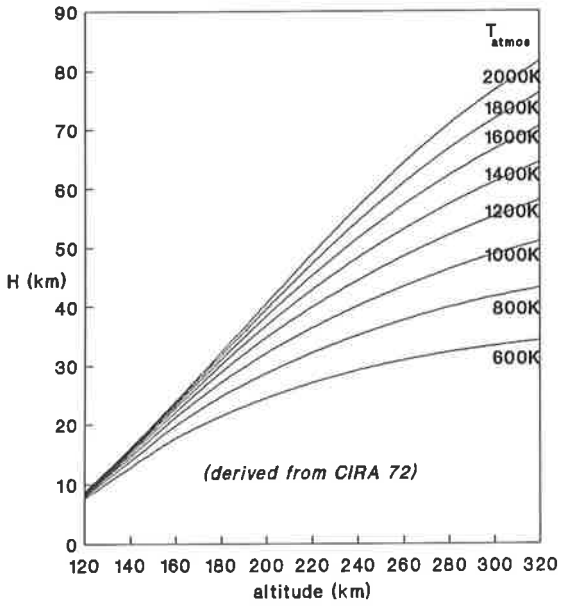

Figure 2. Scale height variation

From inspection we can see that the expression is independent of density or satellite parameters. The density scale height H is plotted in figure 2 and illustrates its relative consistency compared to the neutral density and gives a clue to the robustness of the King-Hele technique.

The relationship between density and scale height is given as:

$$\rho(t) = \rho_p \exp\left(\frac{r_p - r(t)}{H}\right) \qquad (2)$$

where ρ is the neutral density
r is the distance from the Earth centre (=a for circular orbit)
and the subscript p refers to the perigee (minimum altitude) value.

In the past the density scale height was calculated using the 90 day mean value of the solar activity index $F_{10.7}$. Recent research (Ref. 8) suggests that the daily value of $F_{10.7}$ should also be accounted for in determining H and H_H for use with equation 1 and this practice is followed in these calculations. In addition it is necessary to calculate the factors accounting for the semi-annual variation in density, the effect of altitude oscillation due to Earth gravitational anomalies and the oblate form of the Earth and the atmosphere, and the point in the solar activity cycle at which the lifetime prediction takes place.

Using orbital data derived from the NASA 2 line element sets, reentry predictions for the PION satellites are shown in figures 3 and 4. Also plotted are the levels of solar activity (daily and 90-day mean) prevailing at the times of the orbit determinations. The actual reentry epochs of the satellites are shown as Δ in the figures.

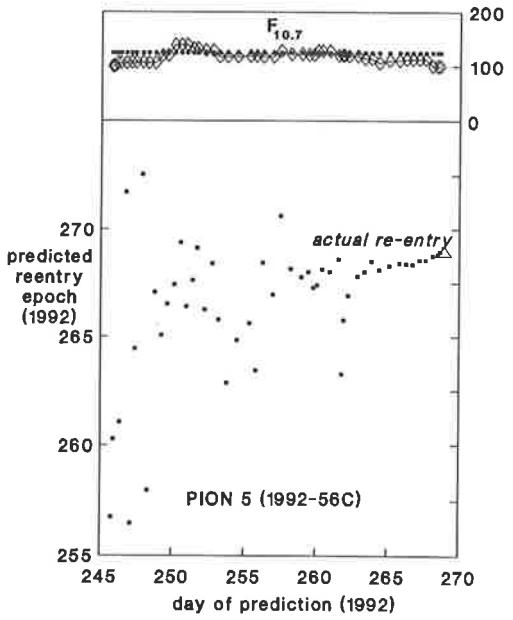

Figure 3. Reentry prediction for PION 5

It can be seen that the predictions derived using the technique show relatively good agreement with the actual reentry but also that there is a substantial degree of dispersion from the general trend. This dispersion is similar in form to the behaviour exhibited during the reentry of the Salyut 7/Kosmos 1686 space station which encountered large instantaneous increases in the $F_{10.7}$ index. However inspection of figures 3

and 4 suggest that this is not the case for the PION predictions.

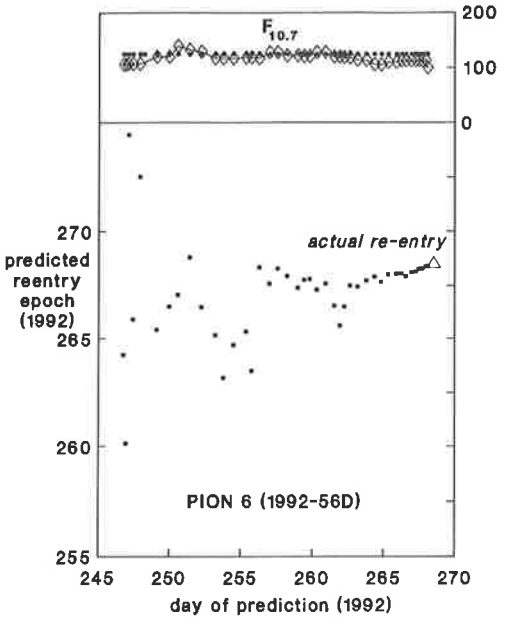

Figure 4. Reentry prediction for PION 6

Limited detective work identifies an alternative culprit. NOAA reported that there were substantial geomagnetic substorms in the lower atmosphere during the period from when the PION satellites were launched and their final reentry epochs. Figure 5 shows the variation of the solar activity and the planetary index a_p with time for this period.

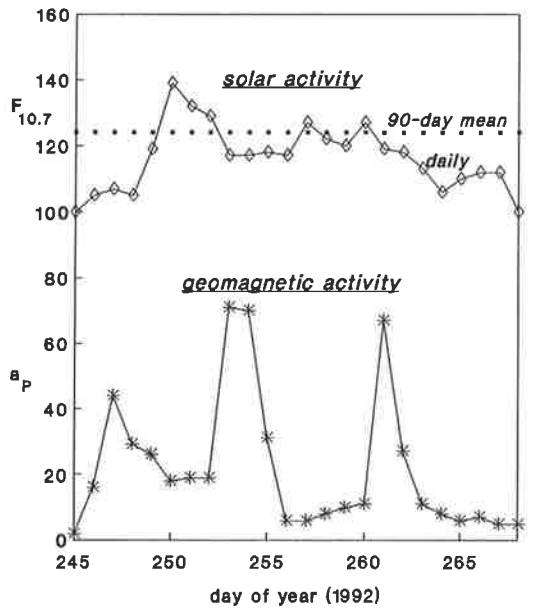

Figure 5. Solar/atmospheric indices during reentry phase

Comparison of figure 5 with figures 3 and 4 show the exact phasing of the reentry prediction dispersions from the actual epoch ▵, with the recorded high levels of a_p. It is apparent that these sudden storms in the lower altitude regions are producing higher densities than would normally be expected under quiescent conditions.

But what is the mechanism by which these storms are affecting the reentry predictions?. The mean motion and its rate of change of mean motion recorded for the PION satellites are plotted in figures 6 and 7, and 8 and 9 respectively.

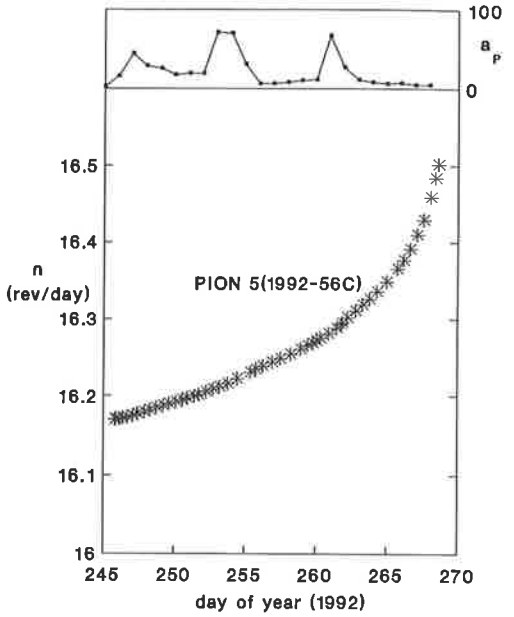

Figure 6. Variation of mean motion for PION 5

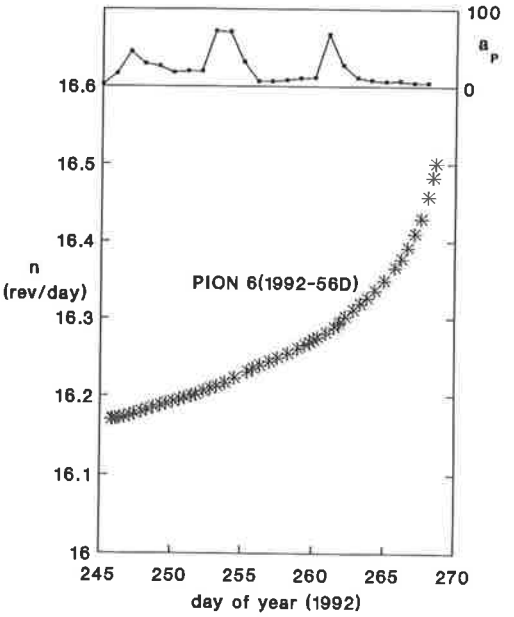

Figure 7. Variation of mean motion for PION 6

Although the mean motion for both PION 5 and PION 6 does not appear to be affected by the substorms, it is apparent that the rate of change of the mean motion is very sensitive to the recorded fluctuations in the planetary index. As the King-Hele technique relies on the rate of change of mean motion to imply the satellite ballistic coefficient and the general density profile that it is encountering along its trajectory, these transient fluctuations imply a steady state large scale increase in neutral density. This in turn leads to a decrease in the predicted orbital lifetime for a satellite with a particular mean motion n.

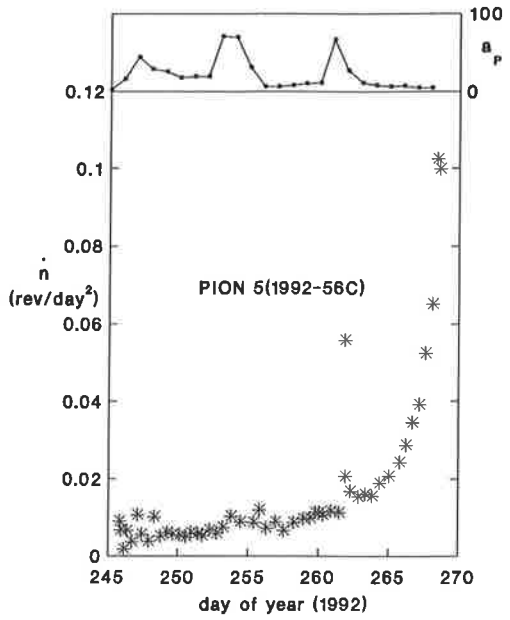

Figure 8. Variation of rate of change of n for PION 5

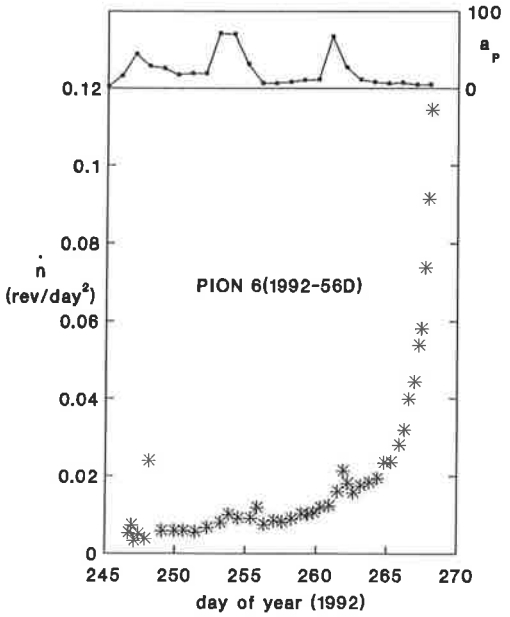

Figure 9. Variation of rate of change of n for PION 6

By their very nature the occurrence of these storms cannot be predicted in advance. We therefore appear to have reached an impasse in our quest to accurately predict the orbital lifetime using this technique. However unlike the increases in the solar activity index $F_{10.7}$, the increases in the planetary index a_p are only transient. Their influence on the trajectory is apparently only restricted to a day or two and therefore the general trend in the trajectory evolution is effectively unaltered. Two options are available therefore to overcome this problem. The first is to monitor the substorm activity and reject trajectory observations on days of high activity. This is not as unsatisfactory as it might first appear because the only time when the storms will exert a direct and lasting influence on the orbital lifetime in on the final few revolutions. The orbit analyst will know when this is the case and can accommodate the a_p fluctuations accordingly. The second solution is to impose some form of smoothing on the rate of change of mean motion values used. In order to counter the influence of the storms this smoothing would need to be carried out over a relatively long period (weeks) or some weighting function would need to be applied. The relative merits of these and alternative solutions are candidates for future research topics.

3. DENSITY DURING GEOMAGNETIC STORMS

The sensitivity of the PION trajectory evolution to the storm activity highlighted above can be turned to our advantage. Unlike most objects which are the subject of reentry predictions, the general configurations of the PION satellites are well characterised:

Shape: *spherical*
Size: *33cm diameter*
Mass: *50 kg*

Therefore it is possible to derive values of the atmospheric density directly from the observed orbital evolution. King-Hele (Ref. 5) has shown that for a satellite moving in a circular orbit within an atmosphere the neutral density ρ is given by:

$$\rho = -\left(\frac{m\,\dot{T}}{3\pi\, a\, S\, C_D}\right) \qquad (3)$$

where m is the mass of the satellite
T is the orbital period
S is the profile area of the satellite ($=\frac{1}{4}\pi d^2$, d= diameter of sphere)
C_D is the aerodynamic drag coefficient.

A problem normally encountered with reentry prediction techniques which seek to directly model the atmospheric density and satellite parameters (special perturbation techniques) is characterisation of the drag coefficient C_D. This is sensitive to the orientation of the vehicle, its shape and the manner in which atmospheric molecules interact with the surface of the satellite. Even if the instantaneous orientation of the vehicle is known the so-called *gas-surface interaction* is not well defined. The phenomenon is known to lie between the two extremes of diffuse and specular reflection although recent analyses (Ref.9) suggest that it lies close to the diffuse case. In the case of the PION satellites, all these problems are bypassed. First the spherical shape of the PION satellites makes attitude information unnecessary. The second and fortunate coincidence is that the spherical shape is relatively insensitive to the *gas-surface interaction*. Bird (Ref. 10) gives an expression for the free molecular drag coefficient of a spherical object:

$$C_D = \frac{2s^2+1}{\sqrt{\pi}s^3}\exp(-s^2)+\frac{4s^4+4s^2-1}{2s^4}\mathrm{erf}(s)+\frac{2(1-\epsilon)\sqrt{\pi}}{3s}\sqrt{\frac{T_w}{T_\infty}} \qquad (4)$$

where s is the ratio of the satellite velocity (relative to the atmosphere) to the random thermal velocity of the atmospheric molecules
ϵ is the fraction of molecules which exhibit specular

reflection

T_w/T_∞ is the temperature ratio of the satellite surface to the temperature of the atmosphere.

The drag coefficient C_D is calculated for a spherical satellite and plotted in figure 10. The molecular speed ratio s relevant to the PION satellites during the period of observation is between 9 and 13, towards what is termed the hyperthermal limit. It is apparent that even for the two extremes of diffuse and specular reflection, the value of C_D is of the order of 2.1 and it is this value that we will use in the following analysis.

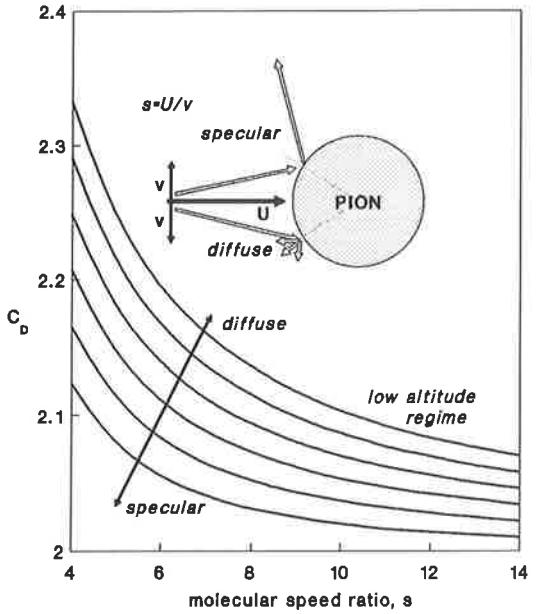

Figure 10. Drag coefficient for spherical satellite

The mean neutral density encountered by the PION satellites along their trajectories is calculated (assuming the quoted values of satellite mass and dimension) and plotted in figures 11 and 12. It is apparent that the density along the trajectory increased by almost an order of magnitude as the PION satellites passed through the storm regions.

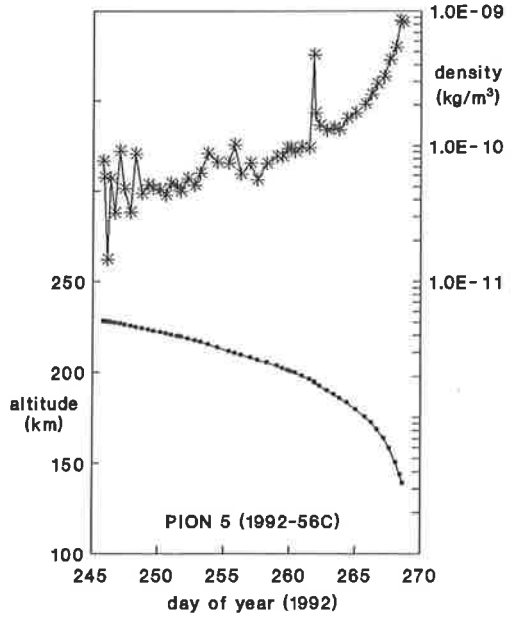

Figure 11. Density derived from change in T (PION 5)

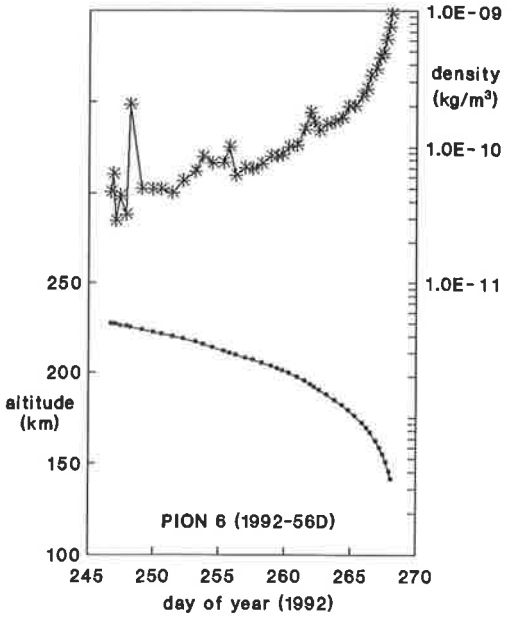

Figure 12. Density derived from change in T (PION 6)

It is also clear from the figures that the density profile along the unperturbed trajectory follows the classical exponential form with altitude and settles down relatively quickly following a substorm event. This would appear to reinforce our previous assertion that rejection of orbit data derived during storm events is valid for reentry predictions as they do not have a lasting effect on the trajectory.

4. CONCLUSIONS

Analyses of the NASA 2 line elements sets derived for the PION 5 and 6 satellites illustrate the influence of geomagnetic substorms on the trajectories of objects in low Earth orbit. These effects are found to be transient, but the short term increases in neutral density lead to substantial increases in the instantaneous rate of orbit decay which can perturb lifetime predictions from the actual reentry epoch. A possible strategy for overcoming this problem is to reject orbit data derived during storm activity. As the storms are short lived, this will still permit orbital lifetime calculations to be carried out on a sufficiently regular basis to ensure accurate reentry predictions.

5. ACKNOWLEDGEMENT

This research is funded under agreement ROAME ATS 7 funded by the British National Space Centre.

6. REFERENCES

1. Walker, D.M.C., The Last 14 Days Of Skylab 1: Orbit Determination And Analysis. *Royal Aerospace Establishment Technical Report* 82067, 1982

2. Crowther, R., Debris Reentry Prediction: Salyut 7/Kosmos 1686. *Proceedings Of International Workshop On Salyut 7/Kosmos 1686 Reentry*, ESOC, Darmstadt (D), April 1991, ESA Special Publication 345 pp. 51-56.

3. Mehrholz, D., Magura, K., Radar Tracking And Observation Of 'Noncooperative' Space Objects Due To Reentry Of Salyut 7/ Kosmos 1686. *Proceedings Of International Workshop On Salyut 7/Kosmos 1686 Reentry*, ESOC, Darmstadt (D), April 1991, ESA Special Publication 345 pp. 1-8.

4. *COSPAR International Atmosphere 1972 (CIRA 1972)*. Berlin, Akademie-Verlag (1972).

5. King-Hele, D.G., *Satellite Orbits In An Atmosphere*. Blackie, Glasgow and London, 1987.

6. King-Hele, D.G., Methods For Predicting Satellite Orbital Lifetimes. *Royal Aerospace Establishment* Technical Report 77111 (1977)

7. King-Hele, D.G., Walker, D.M.C., The Prediction Of Satellite Lifetimes. *Royal Aerospace Establishment* Technical Report 87030 (1987)

8. Crowther, R., Space Debris: Orbit Decay And Reentry Prediction In Theory And Practice. *Advances In The Astronautical Sciences*, vol. 79, pt. 2, pp. 967-982, 1992

9. Crowther, R., Reentry Aerodynamics Derived From Space Debris Trajectory Analysis. *Planetary and Space Science*, vol. 40, no. 5, pp. 641-646, 1992

10. Bird, G.A., *Molecular Gas Dynamics*. Oxford University Press, Oxford UK.